

AD-A236 228



REPORT DOCUMENTATION PAGE

Form Approved
OMB No. 0704-0188

Information is estimated to average 1 hour per response, including the time for reviewing instructions, searching existing data sources, gathering and completing the collection of information, and completing and reviewing the collection of information. Send comments regarding this burden estimate or any other aspect of this collection of information, including suggestions for reducing this burden, to Washington Headquarters Services, Directorate for Information Operations and Reports, 1215 Jefferson Davis Highway, Suite 1204, Arlington, VA 22202-4302, and to the Office of Management and Budget, Paperwork Reduction Project (0704-0188), Washington, DC 20503.

1. (ink)

2. REPORT DATE

7 May 1991

3. REPORT TYPE AND DATES COVERED

Final Report/1 Nov 87-31 Oct 90

4. TITLE AND SUBTITLE

A Study of the Angular Diameters of Dust Shells
Around Red Giants

5. FUNDING NUMBERS

61102F/2311/A1

6. AUTHOR(S)

H. Melvin Dyck

7. PERFORMING ORGANIZATION NAME(S) AND ADDRESS(ES)

Univ of Wyoming
Dept of Physics & Astronomy
Laramie, WY 82071

AFOSR-TR-

8. PERFORMING ORGANIZATION
REPORT NUMBER

91 05 26

9. SPONSORING/MONITORING AGENCY NAME(S) AND ADDRESS(ES)

AFOSR/NP
Bolling AFB DC 20332-6448

B10410

10. SPONSORING/MONITORING
AGENCY REPORT NUMBER

AFOSR-88-0057

11. SUPPLEMENTARY NOTES

12a. DISTRIBUTION/AVAILABILITY STATEMENT

Approved for public release; distribution is unlimited.

12b. DISTRIBUTION CODE

13. ABSTRACT (Maximum 200 words)

We report a summary of our observations of the angular diameters of the shells around evolved red giants. Many of these sources are partially resolved with a ground-based 2.4-m telescope. We have concentrated our efforts in the 8 - 13 micron spectral range because this corresponds to the emission excesses observed in the spectra of oxygen-rich stars. These excesses are commonly thought to arise from small "silicate" mineral grains in the circumstellar shells. We have fully resolved the shell structure for the bright supergiant alpha Orionis. A study of the results shows that the opacity of the silicate mineral grains around that star is similar to that inferred for other evolved stars and for the Trapezium.

14. SUBJECT TERMS

15. NUMBER OF PAGES

16

16. PRICE CODE

17. SECURITY CLASSIFICATION
OF REPORT

UNCLASSIFIED

18. SECURITY CLASSIFICATION
OF THIS PAGE

UNCLASSIFIED

19. SECURITY CLASSIFICATION
OF ABSTRACT

UNCLASSIFIED

20. LIMITATION OF ABSTRACT

SAR

AFOSR-TR-88-0057

A STUDY OF THE ANGULAR DIAMETERS OF DUST SHELLS AROUND RED GIANTS

H. M. Dyck and J. A. Benson
Department of Physics and Astronomy
University Station, P.O. Box 3905
University of Wyoming
Laramie, Wyoming 82071

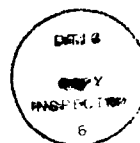
1 May 1991

FINAL REPORT

1 November 1987 - 31 October 1990

Approved for public release; distribution unlimited

Air Force Office of Scientific Research
Department of the Air Force
Bolling Air Force Base, DC 20332-6448



Distribution For	
ALL GR&I	<input checked="" type="checkbox"/>
DTIC Tab	<input type="checkbox"/>
Unclassified	<input type="checkbox"/>
Justification	
By	
Distribution/	
Availability Codes	
Dist	Avail and/or Special
A-1	

91 6 6 017

91-01391



REPORT DOCUMENTATION PAGE

Form Approved
OMB No. 0704-0188

1a. REPORT SECURITY CLASSIFICATION UNCLASSIFIED			1b. RESTRICTIVE MARKINGS N/A		
2a. SECURITY CLASSIFICATION AUTHORITY N/A			3. DISTRIBUTION / AVAILABILITY OF REPORT UNLIMITED DISTRIBUTION		
2b. DECLASSIFICATION / DOWNGRADING SCHEDULE N/A					
4. PERFORMING ORGANIZATION REPORT NUMBER(S)			5. MONITORING ORGANIZATION REPORT NUMBER(S) AFOSR-TR-88-0057		
6a. NAME OF PERFORMING ORGANIZATION Dept. of Physics & Astronomy		6b. OFFICE SYMBOL (if applicable)	7a. NAME OF MONITORING ORGANIZATION Air Force Office of Scientific Research		
6c. ADDRESS (City, State, and ZIP Code) P.O. Box 3905, University Station University of Wyoming Laramie, WY 82071			7b. ADDRESS (City, State, and ZIP Code) Bolling Air Force Base DC 20332-6448		
8a. NAME OF FUNDING / SPONSORING ORGANIZATION AFOSR		8b. OFFICE SYMBOL (if applicable)	9. PROCUREMENT INSTRUMENT IDENTIFICATION NUMBER AFOSR-88-0057		
8c. ADDRESS (City, State, and ZIP Code) Bolling Air Force Base DC 20332-6448			10. SOURCE OF FUNDING NUMBERS		
			PROGRAM ELEMENT NO.	PROJECT NO.	TASK NO.
			WORK UNIT ACCESSION NO.		
11. TITLE (Include Security Classification) A STUDY OF THE ANGULAR DIAMETERS OF DUST SHELLS AROUND RED GIANTS					
12. PERSONAL AUTHOR(S) H. M. DYCK & J. A. BENSON					
13a. TYPE OF REPORT FINAL		13b. TIME COVERED FROM 11/1/87 TO 10/31/90		14. DATE OF REPORT (Year, Month, Day) 1991 May 1	
15. PAGE COUNT 34					
16. SUPPLEMENTARY NOTATION					
17. COSATI CODES			18. SUBJECT TERMS (Continue on reverse if necessary and identify by block number)		
FIELD	GROUP	SUB-GROUP	Final Technical Report		
19. ABSTRACT (Continue on reverse if necessary and identify by block number) We report a summary of our observations of the angular diameters of the shells around evolved red giants. Many of these sources are partially resolved with a ground-based 2.4-m telescope. We have concentrated our efforts in the 8 - 13 micron spectral range because this corresponds to the emission excesses observed in the spectra of oxygen-rich stars. These excesses are commonly thought to arise from small "silicate" mineral grains in the circumstellar shells. We have fully resolved the shell structure for the bright supergiant alpha Orionis. A study of the results shows that the opacity of the silicate mineral grains around that star is similar to that inferred for other evolved stars and for the Trapezium.					
20. DISTRIBUTION / AVAILABILITY OF ABSTRACT <input checked="" type="checkbox"/> UNCLASSIFIED/UNLIMITED <input type="checkbox"/> SAME AS RPT <input type="checkbox"/> DTIC USERS			21. ABSTRACT SECURITY CLASSIFICATION UNCLASSIFIED		
22a. NAME OF RESPONSIBLE INDIVIDUAL			22b. TELEPHONE (Include Area Code)		22c. OFFICE SYMBOL

TABLE OF CONTENTS

I. Introduction	4
II. The Observations and Models	4
Table 1	5
Table 2	6
III. The Variation of Angular Diameter with Wavelength	6
Table 3	7
Table 4	7
Table 5	8
Figure 1	9
Figure 2	10
Figure 3	11
IV. Conclusions	12
References	13
Appendix (Figures A1-A20)	14

I. Introduction

It is well known from radiative transfer theory that the physical parameters characterizing a particular source are constrained not only by the flux spectrum but also by the angular size of the source. Fix and Cobb (1988) pointed out that measurements of the angular size as a function of wavelength, in the range from 8 to 13 μm , can be particularly useful to define the opacity of dust in circumstellar shells. For stars on the red giant and asymptotic giant branches of post-main sequence evolutionary tracks, circumstellar shells are the footprint of extensive mass loss. The mass loss process appears to be very common and may be expected to affect both the evolution of the parent star and the equilibrium of the interstellar medium. Unfortunately, for most evolved stars, very little angular size information exists at any wavelength and even less over a range of wavelengths.

We began a program of one-dimensional (1D) speckle interferometry to measure the angular diameters of evolved stars at several wavelengths between about 1 and 13 μm , with special emphasis to the region around 10 μm . This spectral region is close to the maximum of the excess emission radiated by dust in shells around oxygen-rich stars which is generally attributed to thermal radiation from small silicate grains.

Results of our surveys to identify potentially interesting candidate stars have already been published (Dyck et al. 1984; Benson et al. 1989). In this report we present additional observations of a number of the brighter and larger angular sized shells. Both oxygen-rich and carbon-rich stars showing a wide range of shell optical thicknesses have been included in the study. This report is the only forum in which some of the data will ever be published. It is our hope that these data will provide a useful basis for comparison to sophisticated circumstellar shell model predictions.

In addition to our own observations, which make up the bulk of the data presented, we have included estimates of angular diameters taken from other studies. A summary of all stars considered is given in Table 2. In the remainder of the report we describe the observations and the qualitative differences seen from one star to another.

II. The Observations and Models

Our basic speckle scanning technique has already been described (Dyck and Howell 1985; Benson et al. 1989). In Table 1 we have listed the central wavelengths and bandwidths of the spectral passband filters used for the observations. Most of the data were obtained during 1988 and 1989 using the University of Wyoming 2.4-m telescope on Jelm Mountain in southern Wyoming. Some data were obtained earlier at the 3.8-m UKIRT, the 3-m IRTF or the 2.2-m University of Hawaii telescopes on Mauna Kea.

Generally the observations were made by scanning the image along a north-south position angle (PA) but these were supplemented with occasional observations at other PA. In Table 2 we have given a log of the new observations. These are listed in the last column of the table (1) as a figure number (in the Appendix of this report) in which the visibility curves are plotted and (2) as dates (in parentheses) on which the observations were taken.

The data have been plotted in the Appendix, in Figures A1 through A20, as visibility amplitudes, $V(S)$, versus spatial frequency, $S(\text{cycles/arcsec})$. All visibilities have been normalized to unity at $S = 0$. The instrumental and atmospheric response have been removed by dividing the raw source visibility by the corresponding visibility of an unresolved calibrator. Each data set is characterized by the wavelength and PA of the observation, given in parentheses next to the graph. We have shown 1- σ error bars when they exceed the size of the plotted point, where the errors have been determined from the dispersion among numerous independent sets of observations. The standard error of the mean has been adopted.

We have computed simple model fits to the data for the purpose of discussion. These consist either of (1) a single-component Gaussian brightness distribution characterized by an angular size, θ , which is full-width at half maximum intensity (FWHM) or (2) a two-component brightness distribution in which one component is a Gaussian and the other is unresolved. In this latter case θ corresponds to the FWHM of the resolved halo and V_c to the fraction of the flux emitted by the unresolved core source. Although the Gaussian models are not necessarily realistic, they are convenient and, generally, the angular diameters derived from them are scalable in a simple way to angular sizes of more appropriate brightness distributions. Because the models are not fundamental they have not been shown on the visibility graphs. The results of the model fits to our observations are given in Table 3. For the two-component models, we have listed the values of V_c in Table 4. Other estimates of angular size are summarized in Table 5 along with references to the source of the data.

TABLE 1: The spectral filters.

Name	$\lambda_0(\mu\text{m})$	$\Delta\lambda(\mu\text{m})$
J	1.25	0.2
H	1.65	0.3
K	2.2	0.4
L	3.5	0.8
L'	3.8	0.6
M'	4.8	0.5
M	5.0	0.6
-	7.9	1
-	8.7	1
N	10	6
-	10.3	1
-	10.4	1
-	11.4	2
-	12.6	0.8
Q	20	6

TABLE 2: A summary of the stars discussed in this report.

AFGL	Name	Spectrum	Figures & Dates
57	T Cas	M6-M8	
157	CIT 3	C	A1(11-84)
323	S Per	M3 Ia	A9(8-89)
482	-	C	A1(10-81)
489	CIT 5	C4,3	
529	NML Tau	M8-M11	
836	α Ori	M2 Iab	A2(8-87,2-88,1-89), A10(8-88,1-89),A11(1-89), A12(1-85)
1111	VY CMa	M5 Ib	
1381	IRC+10216	C9,5	A6(12-88),A13(1-89), A14(1-89)
1403	CIT 6	C4,3	A15(6-87,1-89)
1606	SW Vir	M7 III	
1706	RX Boo	M8	A7(7-88,8-88),A16(6-88, 8-88,1-89,7-89)
4990	S CrB	M6-M8	
--	X Her	M6	
1858	U Her	M6-M8	
1988	MW Her		
2071	VX Sgr	M4-M8 I	
2205	OH26.5+0.6	M	
2390	IRC+10420	F8 I	
--	HM Sge	M	A1(8-81,6-82)
2465	χ Cyg	S6,2-S10,4	
5447	V1016 Cyg	M3	A3(10-81,11-81,6-82)
2559	BI Cyg	M4	A7(8-88),A17(8-88)
2560	BC Cyg	M4	A18(8-89)
2632	V Cyg	C7,4	
2650	NML Cyg	M6 III	A8(8-88,9-88),A19(8-88, 7-89,8-89)
2781	CIT 13	C	A3(8-81)
2802	μ Cep	M2 Ia	A3(8-81)
3099	-	C	A4(7-85)
3116	IRC+40540	C8,3.5	A4(11-84)
3136	R Aqr	M7	A5(10-81,6-82)
3188	R Cas	M6-M8	A20(1-89)

III. The Variation of Angular Diameter with Wavelength

Ten stars have multiple angular diameter estimates between 2 and 10 μ m; for these the apparent diameter versus wavelength has been plotted in Figures 1 and 2. The data have been taken from the angular sizes tabulated in Tables 3 and 5. It is noteworthy that these data were obtained by both speckle and Michelson interferometry, by different observers and at different

TABLE 3: Model fits to the new observational data.

Star	$\lambda(\mu\text{m})$	PA($^{\circ}$)	$\theta \pm \epsilon$ ($''$)	Star	$\lambda(\mu\text{m})$	PA($^{\circ}$)	$\theta \pm \epsilon$ ($''$)
CIT 3	2.2	0	.21 \pm .02	HM Sge	3.8	0	<.15
S Per	7.9	0	.49 .14	HM Sge	4.8	0	.09 \pm .01
S Per	8.7	0	.25 .13	V1016 Cyg	2.2	0	<.12
S Per	10.4	0	.39 .08	V1016 Cyg	3.8	0	.07 .01
S Per	11.4	0	.35 .11	BI Cyg	3.5	0	<.12
S Per	12.6	0	.40 .03	BI Cyg	5	0	<.09
AFGL 482	3.8	0	<.06	BI Cyg	8.7	0	.14 .04
α Ori	1.25	90	<.04	BI Cyg	10.4	0	.36 .05
α Ori	2.2	0	<.07	BI Cyg	11.4	0	.31 .08
α Ori	3.5	90	<.10	BI Cyg	12.6	0	.20 .04
α Ori	7.9	0	2.4 .1	BC Cyg	7.9	0	.38 .02
α Ori	7.9	90	1.5 .5	BC Cyg	8.7	0	.27 .07
α Ori	8.7	0	2.2 .1	BC Cyg	10.4	0	.37 .09
α Ori	8.7	90	2.6 .1	BC Cyg	11.4	0	.32 .11
α Ori	10.3	0	2.8 .3	BC Cyg	12.6	0	.13 .04
α Ori	10.3	60	2.4 .3	NML Cyg	2.2	0	.08 .02
α Ori	10.3	90	3.2 .2	NML Cyg	3.5	0	.12 .01
α Ori	10.3	120	2.9 .2	NML Cyg	5	0	.19 .01
α Ori	10.3	150	2.7 .2	NML Cyg	7.9	0	.29 .05
α Ori	10.4	0	2.5 .1	NML Cyg	8.7	0	.31 .07
α Ori	10.4	90	1.9 .1	NML Cyg	10.4	0	.30 .05
α Ori	11.4	0	2.4 .1	NML Cyg	11.4	0	.32 .03
α Ori	12.6	0	2.7 .1	NML Cyg	12.6	0	.30 .07
α Ori	20	0	2.3 .3	CIT 13	4.8	0	<.15
CIT 6	8.7	90	.15 .07	μ Cep	4.8	0	.08 .01
CIT 6	10.4	90	.15 .03	AFGL 3099	2.2	0	.16 .04
CIT 6	11.4	90	.23 .03	IRC+40540	2.2	0	.32 .04
CIT 6	12.6	0	.28 .03	R Aqr	2.2	0	3.6 .2
RX Boo	3.5	0	.07 .01	R Aqr	3.8	0	1.8 .1
RX Boo	5	0	<.06	R Aqr	4.8	0	1.4 .1
RX Boo	7.9	0	.15 .03	R Cas	7.9	0	.34 .05
RX Boo	8.7	0	.13 .07	R Cas	8.7	0	.29 .03
RX Boo	10.4	0	.27 .06	R Cas	10.4	0	.47 .03
RX Boo	11.4	0	.27 .06	R Cas	11.4	0	.44 .05
RX Boo	12.6	0	.17 .06	R Cas	12.6	0	.46 .04

TABLE 4: Point source contributions in fully-resolved shells.

Star	$\lambda(\mu\text{m})$	PA($^{\circ}$)	V_s	Star	$\lambda(\mu\text{m})$	PA($^{\circ}$)	V_s
α Ori	7.9	0	0.91	α Ori	10.4	0	0.51
α Ori	7.9	90	0.94	α Ori	10.4	90	0.61
α Ori	8.7	0	0.85	α Ori	11.4	0	0.57
α Ori	8.7	90	0.87	α Ori	12.6	0	0.71
α Ori	10.3	0	0.55	α Ori	20	0	0.00
α Ori	10.3	60	0.64	R Aqr	2.2	0	0.90
α Ori	10.3	90	0.67	R Aqr	3.8	0	0.83
α Ori	10.3	120	0.56	R Aqr	4.8	0	0.83
α Ori	10.3	150	0.48	-----	-----	--	----

Table 5: A Summary of Gaussian FWHM from Other Studies

Star	λ	PA	$\Theta \pm \epsilon (")$	Ref	Star	λ	PA	$\Theta \pm \epsilon (")$	Ref
T Cas	10 μ m	0°	0.26 \pm .01	1	IRC+10420	2.2 μ m	0°	0.07 \pm .01	2
S Per	10 μ m	0°	0.30 \pm .05	1		2.2 μ m	90°	0.07 \pm .01	2
CIT 5	3.8 μ m	0°	<.06	2		3.8 μ m	0°	0.16 \pm .02	2
	4.8 μ m	0°	0.07 \pm .02	2		3.8 μ m	90°	0.12 \pm .01	2
NML Tau	3.8 μ m	0°	<.06	2		4.8 μ m	0°	0.19 \pm .01	2
α Ori	10 μ m	0°	2.7 \pm .1	1		4.8 μ m	90°	0.15 \pm .01	2
	11.6 μ m	0°	2.5 \pm .2	3		5 μ m		0.25	4
VY CMa	3.8 μ m	0°	0.12 \pm .02	2		8.4 μ m		0.33	4
	4.8 μ m	0°	0.14 \pm .02	2		8.7 μ m	0°	0.42 \pm .02	7
	5 μ m		0.17	4		9.8 μ m	0°	0.42 \pm .02	7
	8.4 μ m		0.29	4		10.2 μ m		0.33	4
	10.2 μ m		0.58	4		12.5 μ m		0.42	4
	11 μ m		0.48	5	χ Cyg	2.2 μ m	90°	<.06	2
	11.1 μ m		0.50	4		4.6 μ m	90°	0.10 \pm .02	6
CIT 6	2.2 μ m	0°	0.06 \pm .01	2		4.8 μ m	0°	0.11 \pm .02	2
	2.2 μ m	90°	0.08 \pm .01	2		4.8 μ m	0°	0.08 \pm .01	2
	3.8 μ m	0°	0.10 \pm .02	2		5 μ m		<.08	4
	4.8 μ m	0°	0.14 \pm .02	2		10 μ m	0°	0.27 \pm .05	1
	5 μ m		0.12	4		10.2 μ m		>.25	4
	10 μ m	0°	0.33 \pm .01	1	BI Cyg	10 μ m	0°	0.35 \pm .04	1
	10.2 μ m		0.17	4	BC Cyg	10 μ m	0°	0.41 \pm .01	1
	12.5 μ m		0.25	4		3.5 μ m		<.04	4
SW Vir	2.4 μ m	90°	0.09 \pm .01	6	V Cyg	3.8 μ m	0°	<.04	2
	10 μ m	0°	0.28 \pm .05	1		5 μ m		<.04	4
RX Boo	10 μ m	0°	0.29 \pm .01	1		10.2 μ m		0.17	4
SCrB	10 μ m	0°	0.24 \pm .05	1	NML Cyg	2.2 μ m	120°	0.05	8
X Her	10 μ m	0°	0.22 \pm .01	1		2.2 μ m	0°	0.08 \pm .01	2
U Her	4.6 μ m	150°	<.10	6		3.3 μ m	120°	0.09	8
	10 μ m	0°	.26 \pm .05	1		3.5 μ m		0.10	4
MW Her	10 μ m	0°	<.24	1		3.8 μ m	0°	0.14 \pm .02	2
VX Sgr	2.2 μ m	0°	0.05 \pm .01	2		4.7 μ m	120°	0.12	8
	3.8 μ m	0°	0.10 \pm .01	2		4.8 μ m	0°	0.19 \pm .02	2
OH26.5+0.6	3.8 μ m	0°	0.07 \pm .02	2		4.8 μ m	90°	0.15 \pm .01	2
	3.8 μ m	90°	0.10 \pm .02	2		5 μ m		0.15	4
	4.6 μ m	90°	<.14	6		8.4 μ m		0.33	4
	4.6 μ m	150°	0.15 \pm .05	6		10 μ m	0°	0.37 \pm .04	7
	4.8 μ m	0°	0.16 \pm .02	2		10 μ m	0°	0.36 \pm .02	1
	4.8 μ m	90°	0.11 \pm .02	2		10.2 μ m		0.33	4
	8.7 μ m	0°	<.2	7		11.1 μ m		0.33	4
	9.8 μ m	0°	0.50 \pm .02	7		12.5 μ m		0.33	4
					R Cas	10 μ m	0°	0.33 \pm .01	1
					μ Cep	8.4 μ m		<.08	4
						10 μ m	0°	0.37 \pm .05	1
						10.2 μ m		0.21	4
						12.5 μ m		0.21	4

Reference Key:

- 1 = Benson *et al.* (1989) 2 = Dyck *et al.* (1984)
 3 = Howell *et al.* (1981) 4 = Low (1979)
 5 = Sutton *et al.* (1977) 6 = Mariotti *et al.* (1983)
 7 = Fix and Cobb (1988) 8 = Sibille *et al.* (1979)

observatories although, in general the agreement among the observations is very good. A specific example is the case of NML Cyg, the data for which are plotted in Figure 2. There is very little scatter in the data indicating that all observers were measuring the same quantity and that there is no evidence that NML Cyg varies. This is in contrast to the observations of IRC+10216 which has been shown to be strongly variable (in angular diameter) at $2.2\ \mu\text{m}$ (Dyck et al. 1991).

All the plotted data in Figures 1 and 2 show a common feature, namely, that the apparent diameter increases with increasing wavelength. This correlation has been previously noted (McCarthy 1979; Dyck et al. 1984) and may be explained principally by the temperature variation in the extended shell (see, e.g., Rowan-Robinson and Harris 1982; Bedijn 1987). It also depends upon the optical depth in the shell and to what extent the flux from the underlying star contaminates the measurement (Dyck et al. 1984).

There are some differences among the ten stars in the details of the wavelength dependence of the angular diameter. CIT 6, the one carbon star shown in the figures, exhibits a generally slower increase of angular diameter between the near infrared ($1\text{--}5\ \mu\text{m}$) and $10\ \mu\text{m}$ than do the oxygen-rich stars. This probably results from differences in the composition of the dust in the respective envelopes: Pure carbon dust does not show the prominent, broad opacity enhancement between 8 and $12\ \mu\text{m}$ that is shown by generic silicates (Draine and Lee 1984). Silicon carbide has a feature at $11.3\ \mu\text{m}$ and variable amounts of this material in carbon-star envelopes could change the ratio of near to mid-infrared diameters.

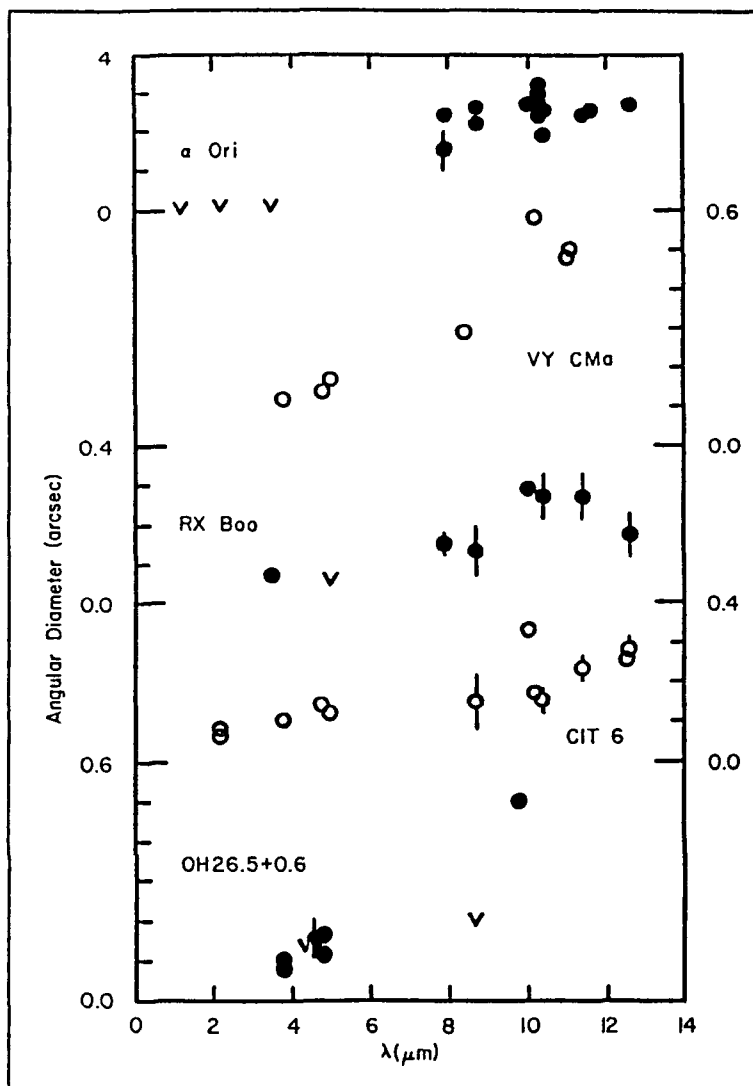


Figure 1: Angular diameter (in arcsec) versus wavelength (in μm) for 5 stars.

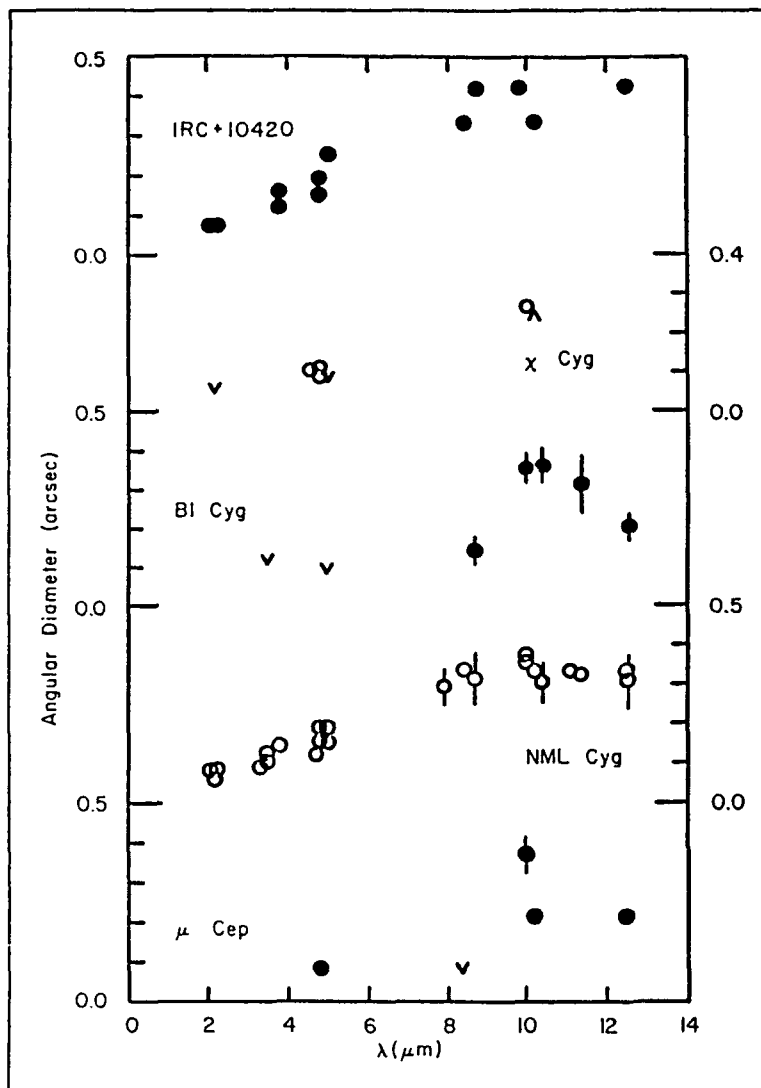


Figure 2: See Figure 1.

Among the oxygen rich stars there appears to be two extremes of behavior within the 8 to 13 μm spectral range. There are stars like α Ori and NML Cyg which show almost no change of angular size over this wavelength range. Most of the stars with detailed 10 μm wavelength dependence data are of this type (although we have not plotted the individual data for all of them). Then there are RX Boo and BI Cyg which apparently do show a change of angular diameter with wavelength around 10 μm . There is no apparent correlation with optical depth in the envelope, with α Ori having the lowest and NML Cyg the greatest 10 μm optical depths. Dyck and Benson (1991) have argued that these disparate results may be explained if it is recognized that α Ori is the only star with a completely resolved

circumstellar shell at 10 μm . For the remaining stars only partial resolution is achieved. Then, for the optically thinner shells (RX Boo and BI Cyg) the apparent variation with wavelength arises from the differing contribution from the underlying star at different wavelengths. The "true" variation of the shell diameter for both optically thin and thick shells appears to be small over this range of wavelengths.

This analysis has shown that the opacity in the circumstellar shell surrounding α Ori is almost identical to that derived by Bedijn (1987) from the constraint that the flux spectrum must be matched in two other red giant stars. By postulating that the dust opacity is identical in all optically thin shells, one may reproduce the detailed behavior of the partially resolved shells around RX Boo and BI Cyg. This form of the dust opacity is reasonably similar to that derived by Gillett et al. (1975) from the presumed optically thin Trapezium emission. The principal

difference is a lower value of the red giant circumstellar opacity at wavelengths near 8.5 μm . We have shown the results from this study in Figure 3, where the individual points are the relative optical depth derived from the observations of α Ori. The opacity adopted by Bedijn (1987) is shown, for comparison, as a solid line; the Trapezium opacity is shown as a dashed line.

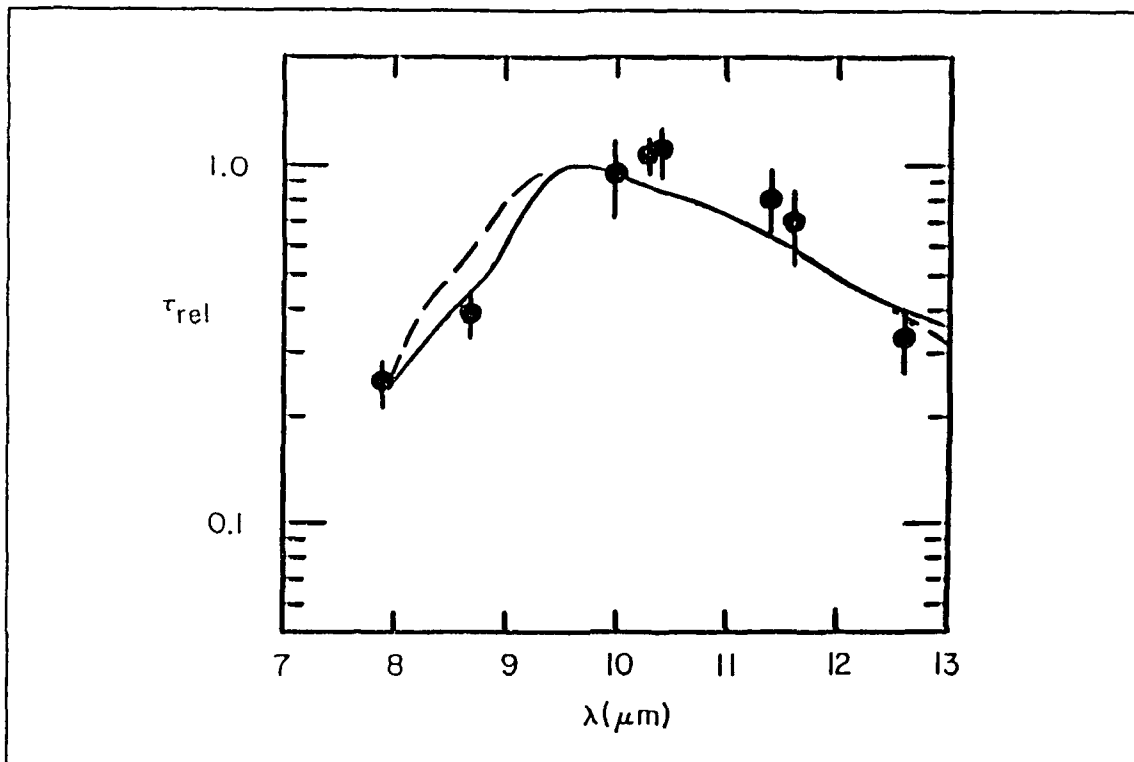


Figure 3: The 10 μm relative optical depth, derived from speckle interferometry of α Orionis. See text for details.

The optically-thicker shells are more problematic because they show no obvious variation of angular diameter with wavelength. This is counter to one's simple expectation if the opacity is similar to that found for the optically-thin shells. If the shell is both physically extensive and optically thick, then one sees, at any wavelength, to an optical depth of approximately $\tau = 1$. Because the opacity varies with wavelength, the physical depth must also vary with wavelength for a fixed τ . Thus the angular diameter must vary with wavelength which is counter to what is observed. We suspect that either the opacity is remarkably different in the two optical depth extremes (see, e.g., the discussion of opacity similarities presented by Bedijn 1987) or that the shells themselves may not be physically very extensive. That is, in the latter case, their radii may be much larger than their thicknesses. This is a problem which appears to be well-established by the observational data but which requires additional theoretical study.

IV. Conclusions

We have shown in this study that circumstellar shell diameter measurements are possible with existing single-mirror ground-based telescopes. A few sources are fully resolved but many are only partially resolved. For the fully-resolved sources it is possible to derive the wavelength dependence of the opacity variation in the shell. A careful study with narrower filters than those employed in our study could delineate this dependence very accurately. This technique would allow theoretical workers to make full use of the power of radiative transfer theory to define empirically the nature of the dust in shells surrounding evolved stars.

Our measurements were carried out with a 2.4-m telescope and the largest ground-based telescopes will gain a factor of two in angular resolution. Inspection of the visibility data plotted in the Appendix suggests to us that telescopes at least a factor of five larger will be needed to increase the sample of fully-resolved sources significantly. This kind of baseline clearly lies in the venue of multiple-telescope interferometry.

REFERENCES

- Bedijn, P.J. 1987, *Astron.Astrophys.* 186, 136.
- Benson, J.A., Turner, N.H. and Dyck, H.M. 1989, *Astron.J.* 97, 1763.
- Draine, B.T. and Lee, H.M. 1984, *Astrophys.J.* 285, 89.
- Dyck, H.M., Zuckerman, B., Leinert, Ch. and Beckwith, S. 1984, *Astrophys.J.* 287, 801.
- Dyck, H.M. and Howell, R.R. 1985, *Proceedings of the SPIE - International Conference on Speckle* 556, 274.
- Dyck, H.M., Benson, J.A., Howell, R.R., Joyce, R.R. and Leinert, Ch. 1991, *Astron.J.*, in press for July.
- Dyck, H.M. and Benson, J.A. 1991, to be submitted to the *Astron.J.*
- Fix, J.D. and Cobb, M.L. 1988, *Astrophys.J.* 329, 290.
- Gillett, F.C., Forrest, W.J., Merrill, K.M., Capps, R.W. and Soifer, B.T. 1975, *Astrophys.J.* 200, 609.
- Howell, R.R., McCarthy, D.W. and Low, F.J. 1981, *Astrophys.J.Letters* 251, L21.
- Low, F.J. 1979, in *IAU Colloquium No. 50: High Angular Resolution Stellar Interferometry*, ed. J. Davis and W.J. Tango (Sydney: Chatterton Astronomy Department, University of Sydney), p.2-1.
- Mariotti, J.-M., Chelli, A., Foy, R., Léna, P., Sibille, F. and Tchountonov, G. 1977, *Astron.Astrophys.* 120, 237.
- McCarthy, D.W. 1979, in *IAU Colloquium No. 50: High Angular Resolution Stellar Interferometry*, ed. J. Davis and W.J. Tango (Sydney: Chatterton Astronomy Department, University of Sydney), p.18-1.
- Rowan-Robinson, M. and Harris, S. 1982, *Mon.Not.Roy.Astron.Soc.* 200, 197.
- Sibille, F., Chelli, A. and Léna, P. 1979, *Astron.Astrophys.* 79, 315.
- Sutton, E.C., Storey, J.W.V., Betz, A.L., Townes, C.H. and Spears, D.L. 1977, *Astrophys.J.Letters* 217, L97.

APPENDIX

In the following graphs we have plotted the normalized amplitude of the complex visibility function, $V(S)$, versus spatial frequency, S , in cycles per arcsecond. The vertical scale is linear with a difference in $V(S)$ of 0.1 between tic marks. Errors are shown only when they exceed the size of the plotted point.

Individual star names appear either at the top of the figure, in which case the entire figure corresponds to that star, or next to the appropriate data set. The parentheses include the filter name or central wavelength and the PA of the observation. The dates of the observations may be found in Table 2.

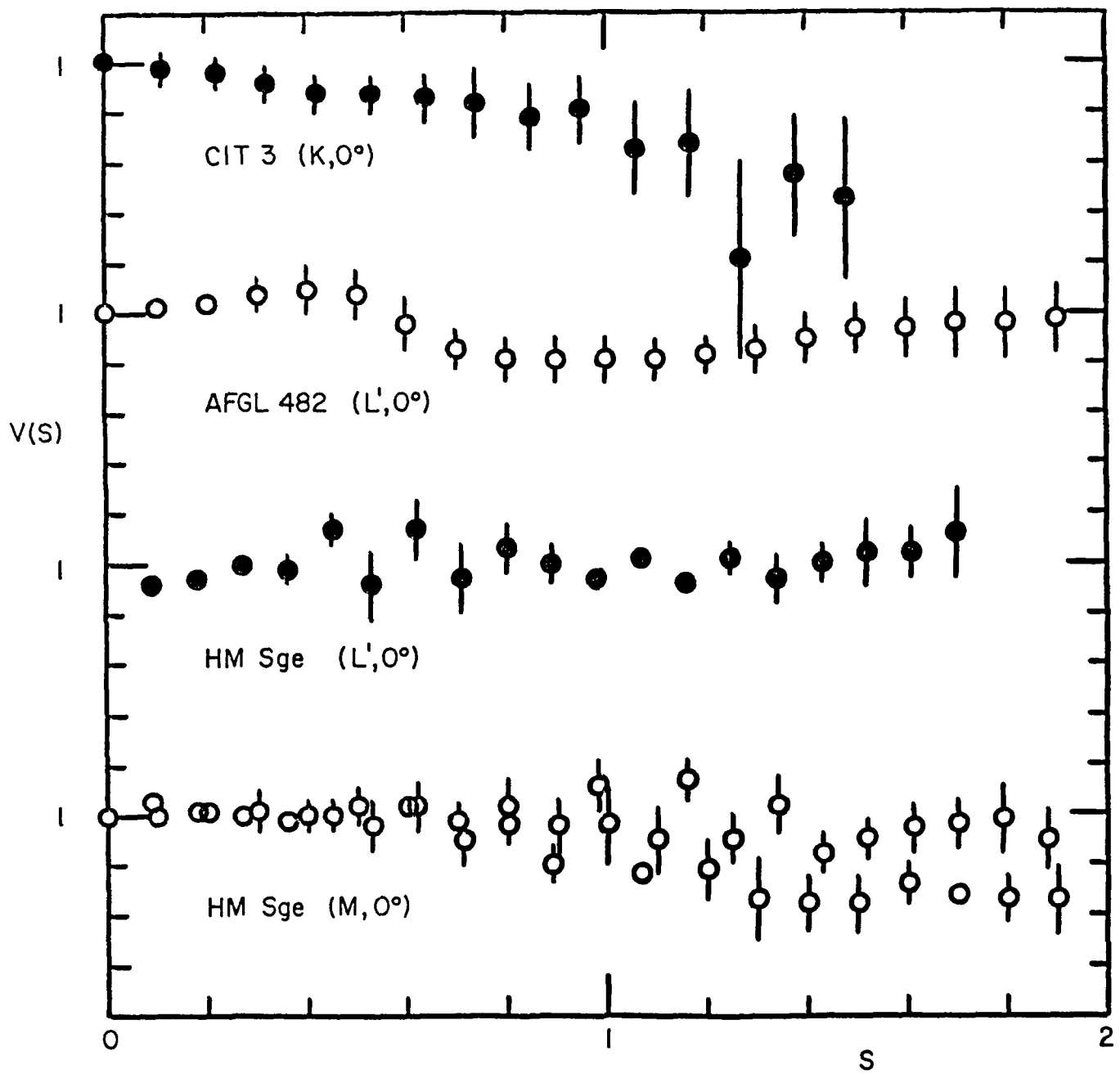


FIGURE A1

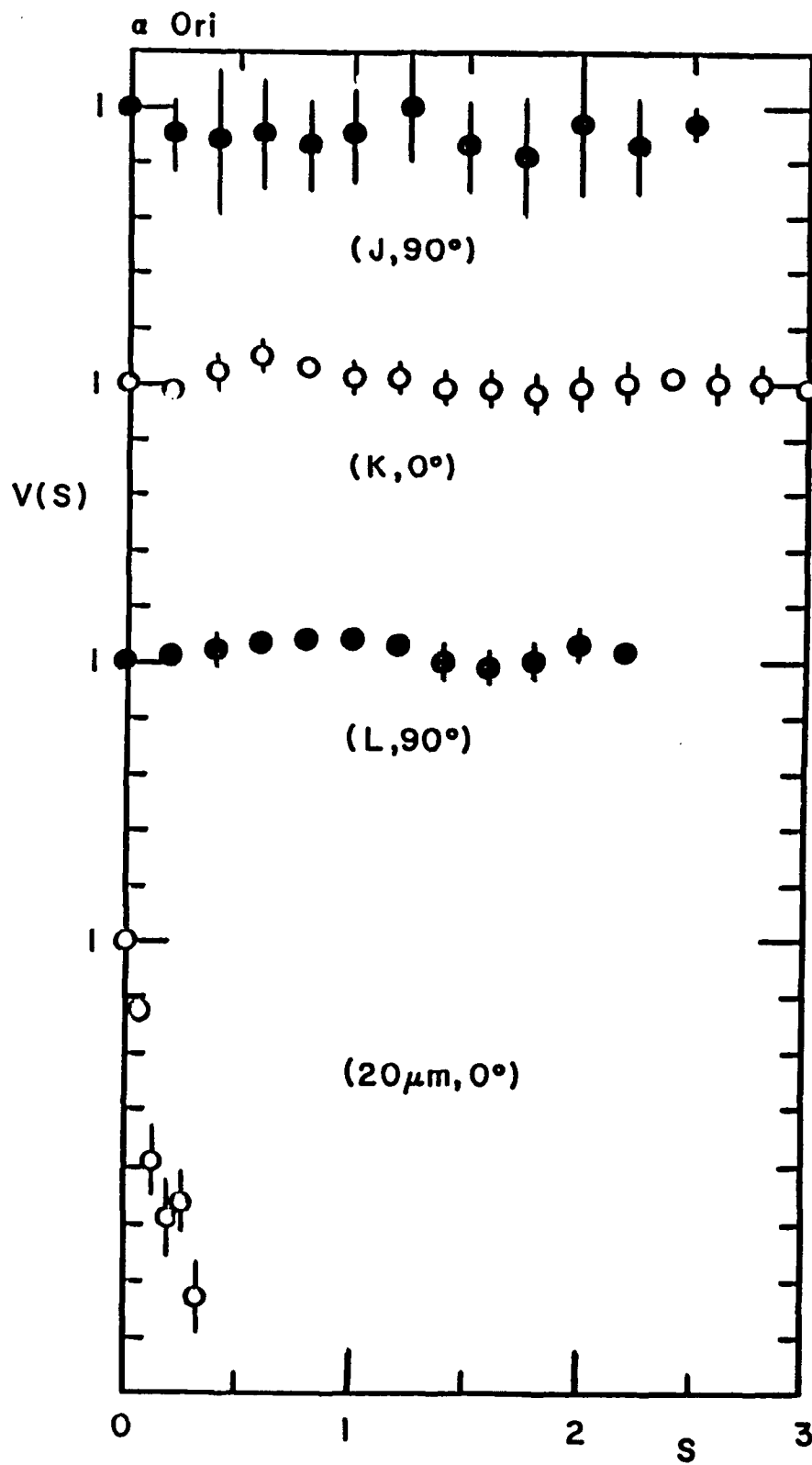


FIGURE A2

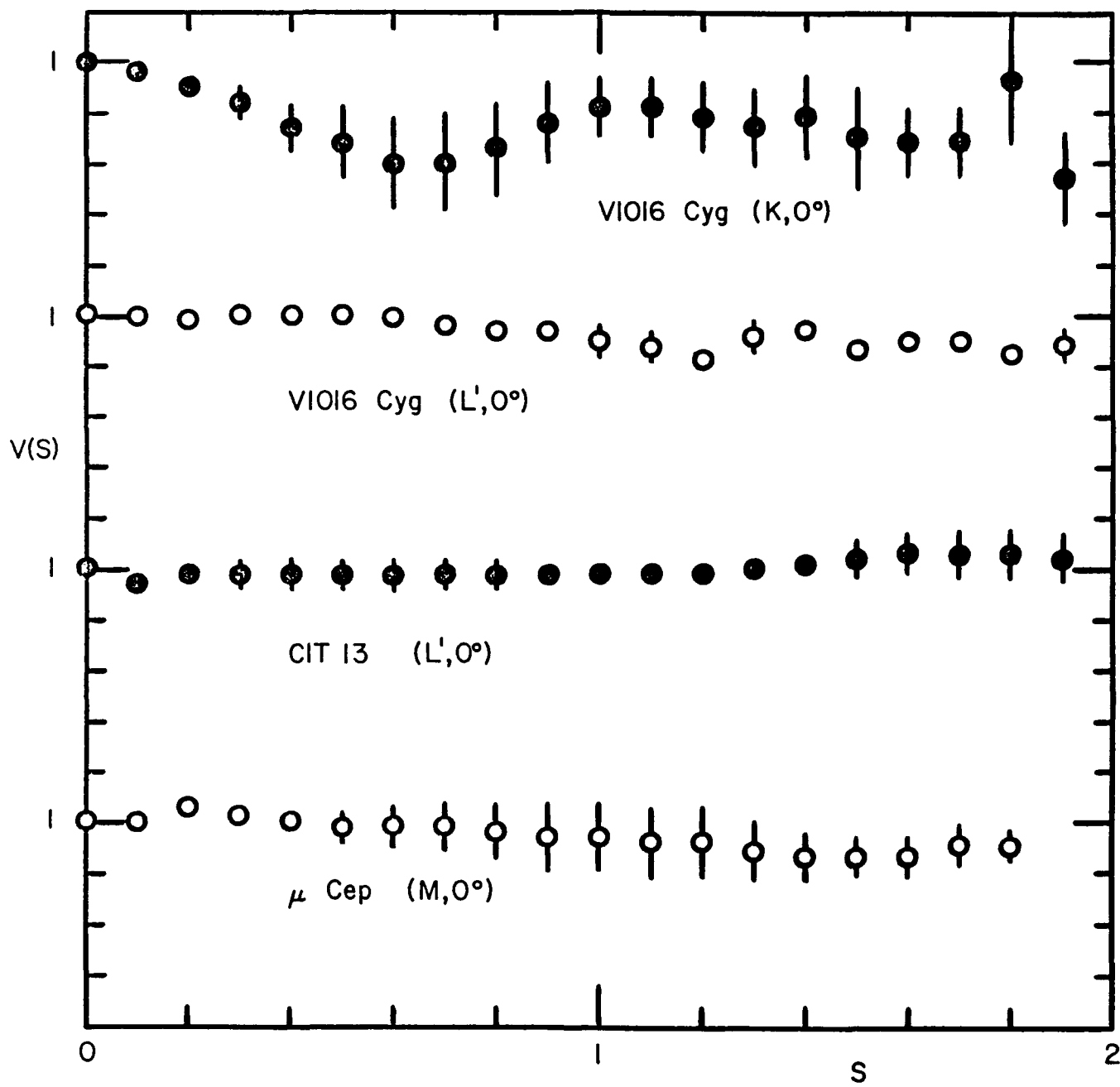


FIGURE A3

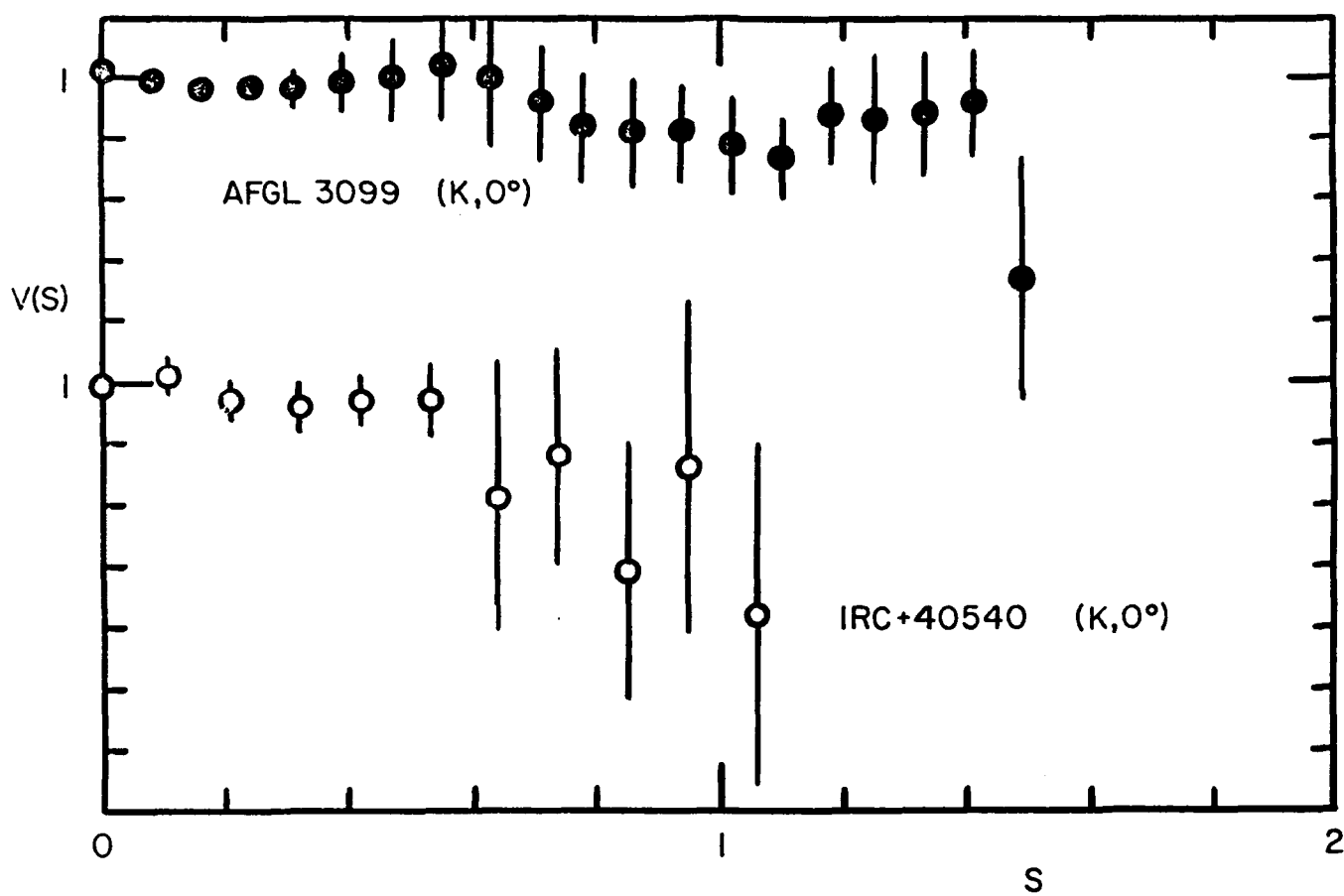


FIGURE A4

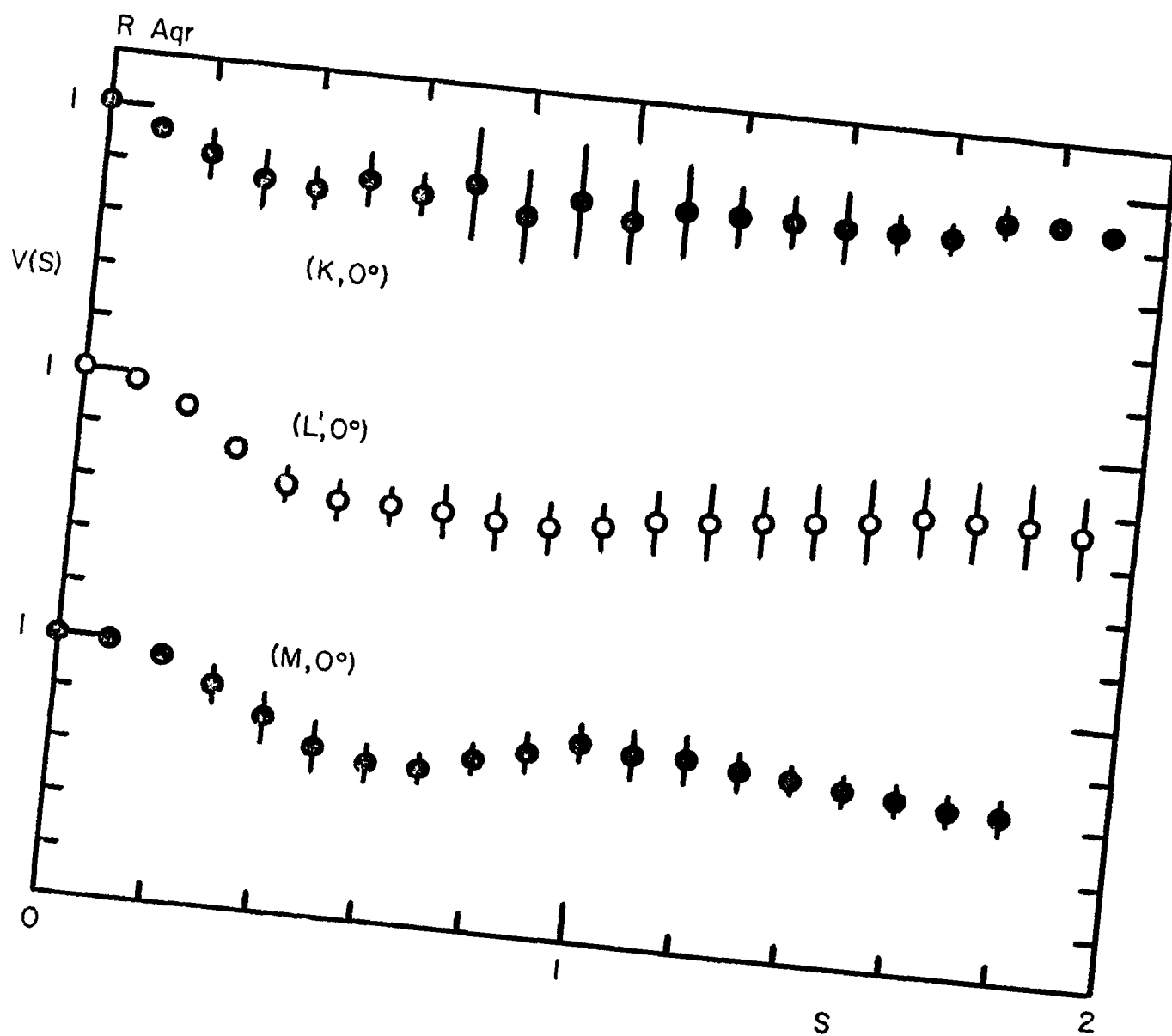
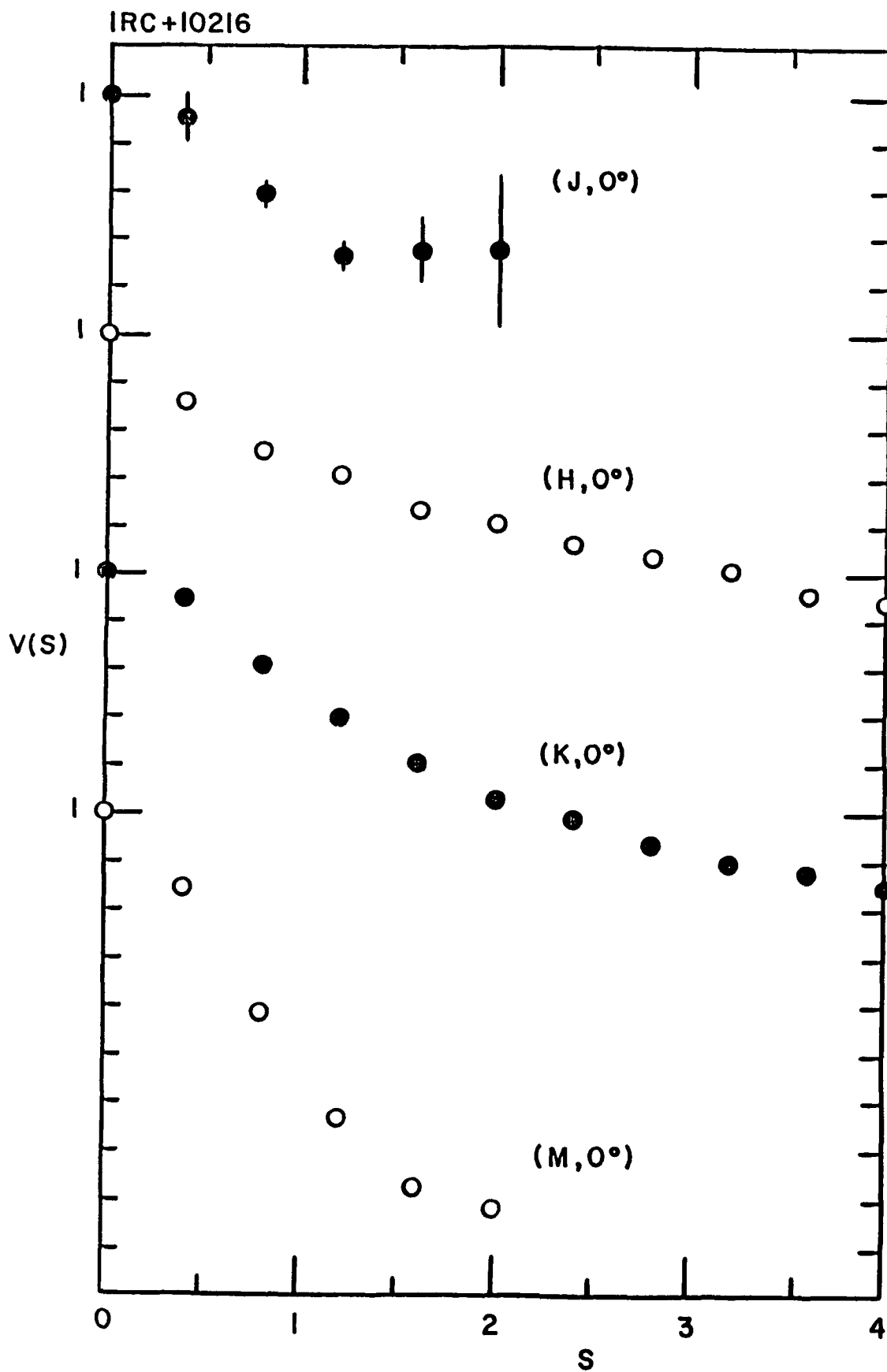


FIGURE A5



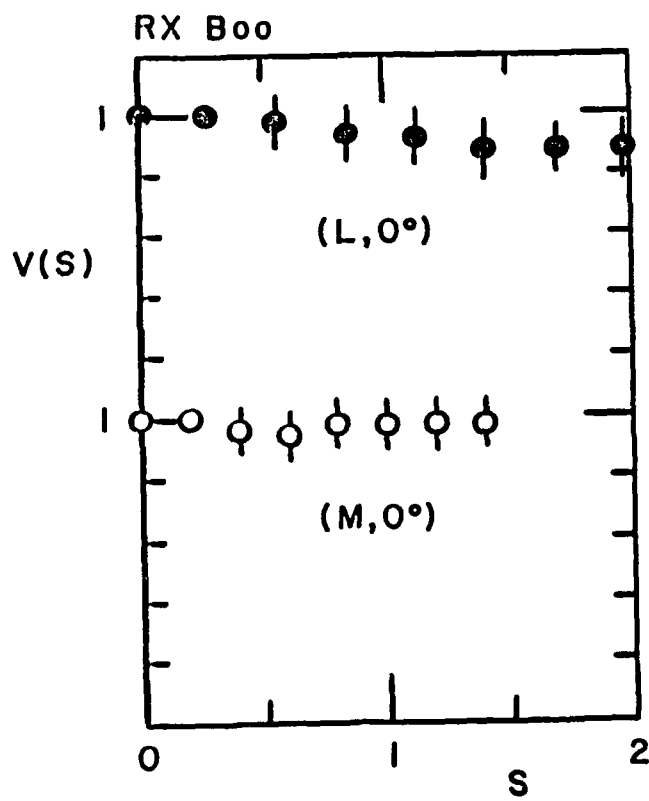
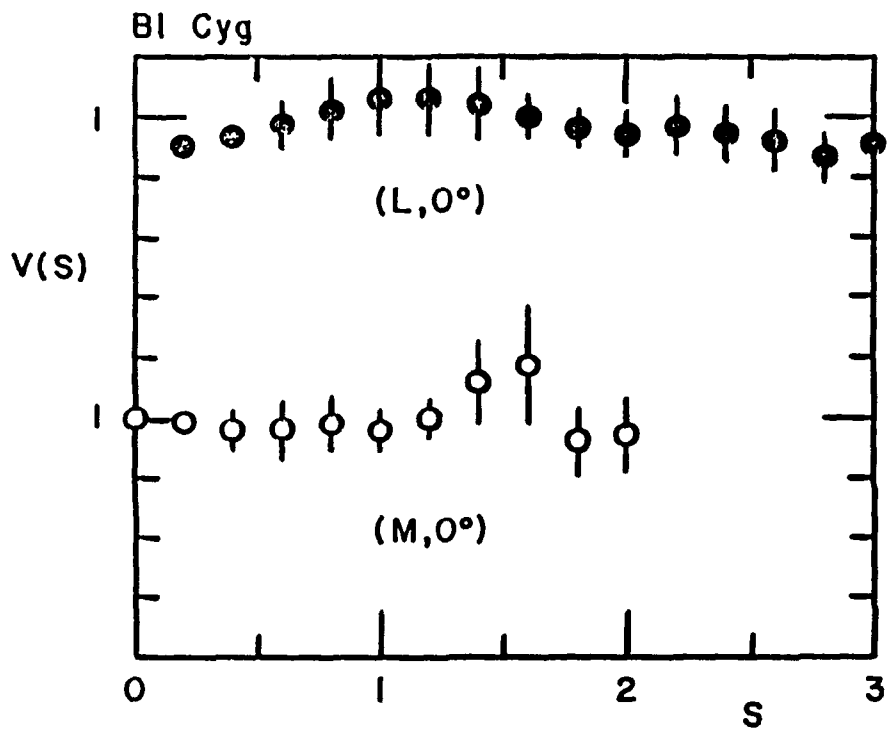
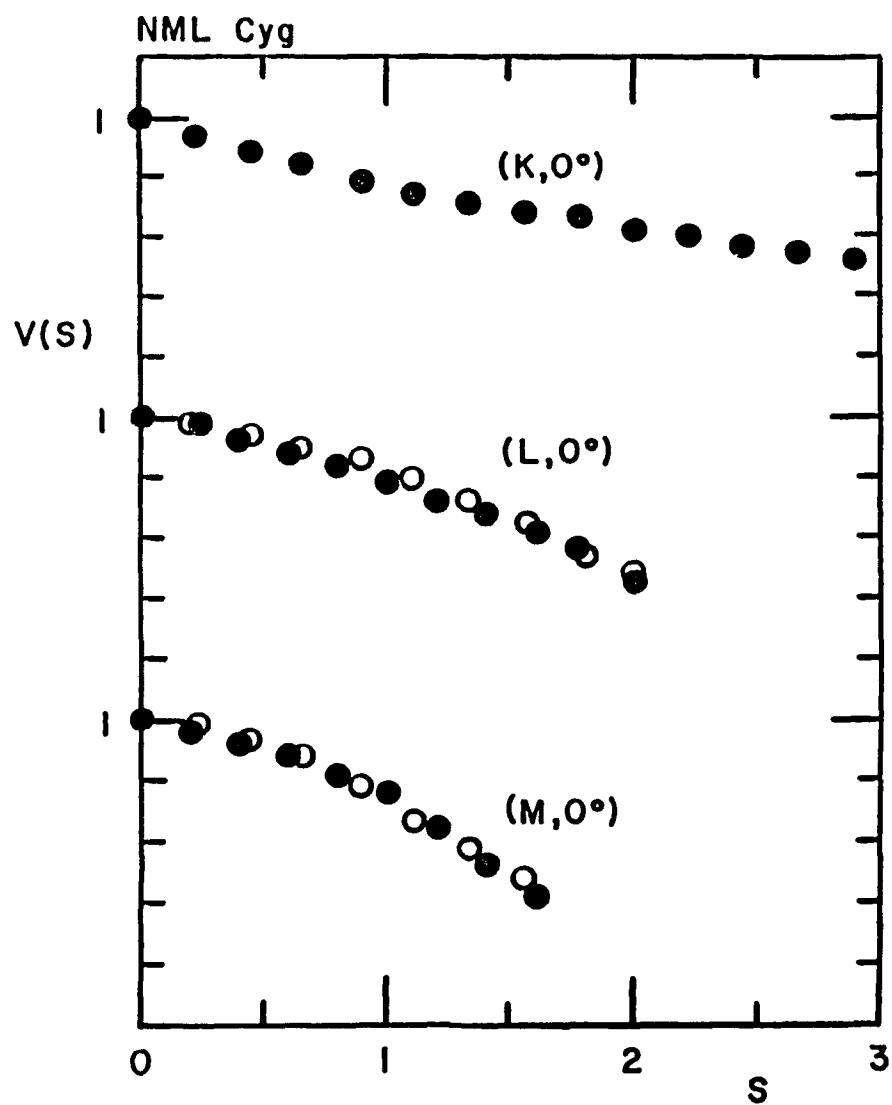


FIGURE A7



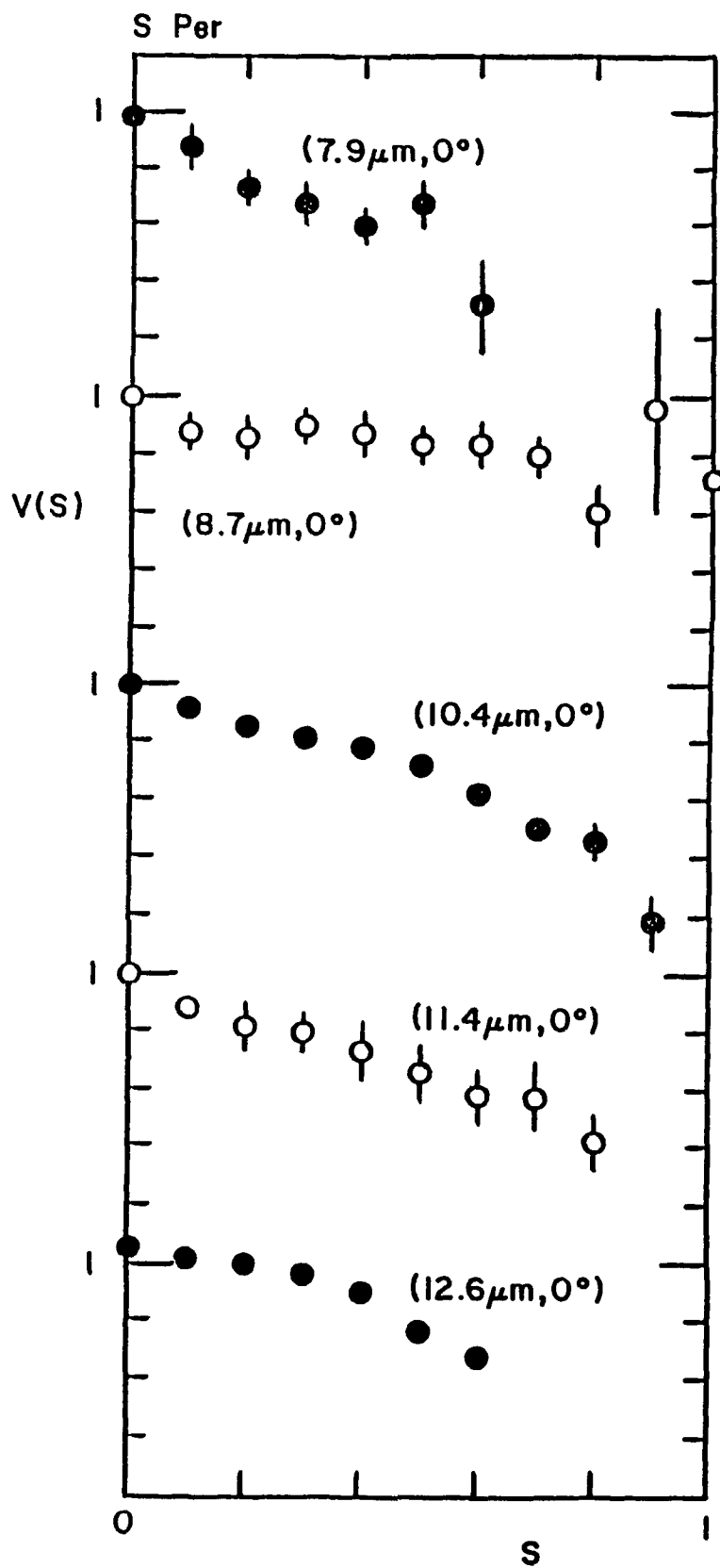
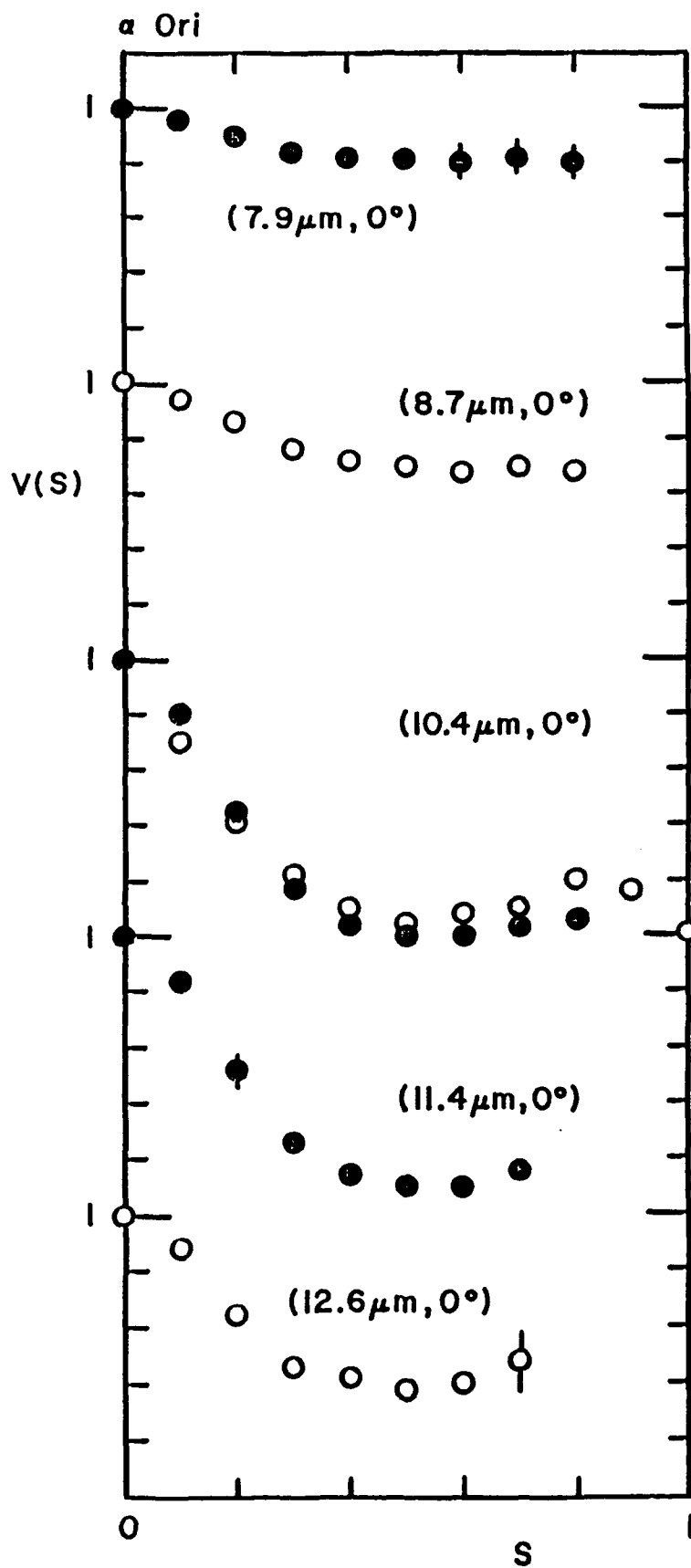


FIGURE A9



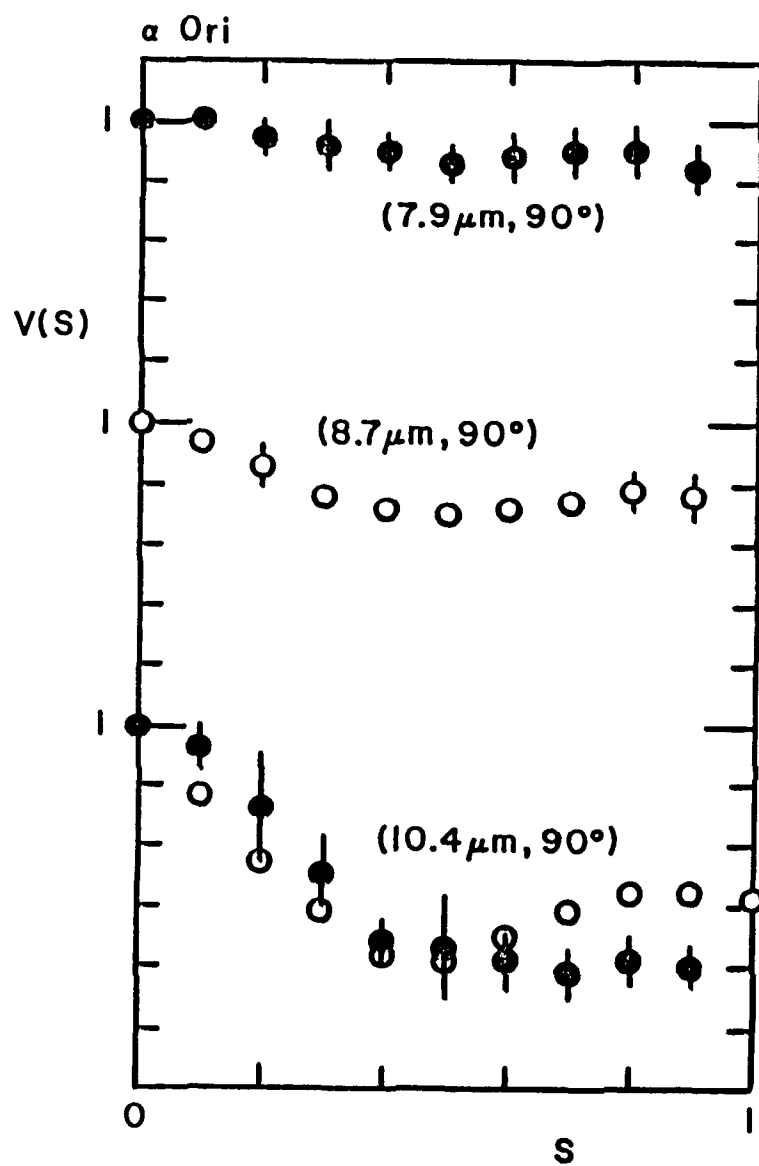
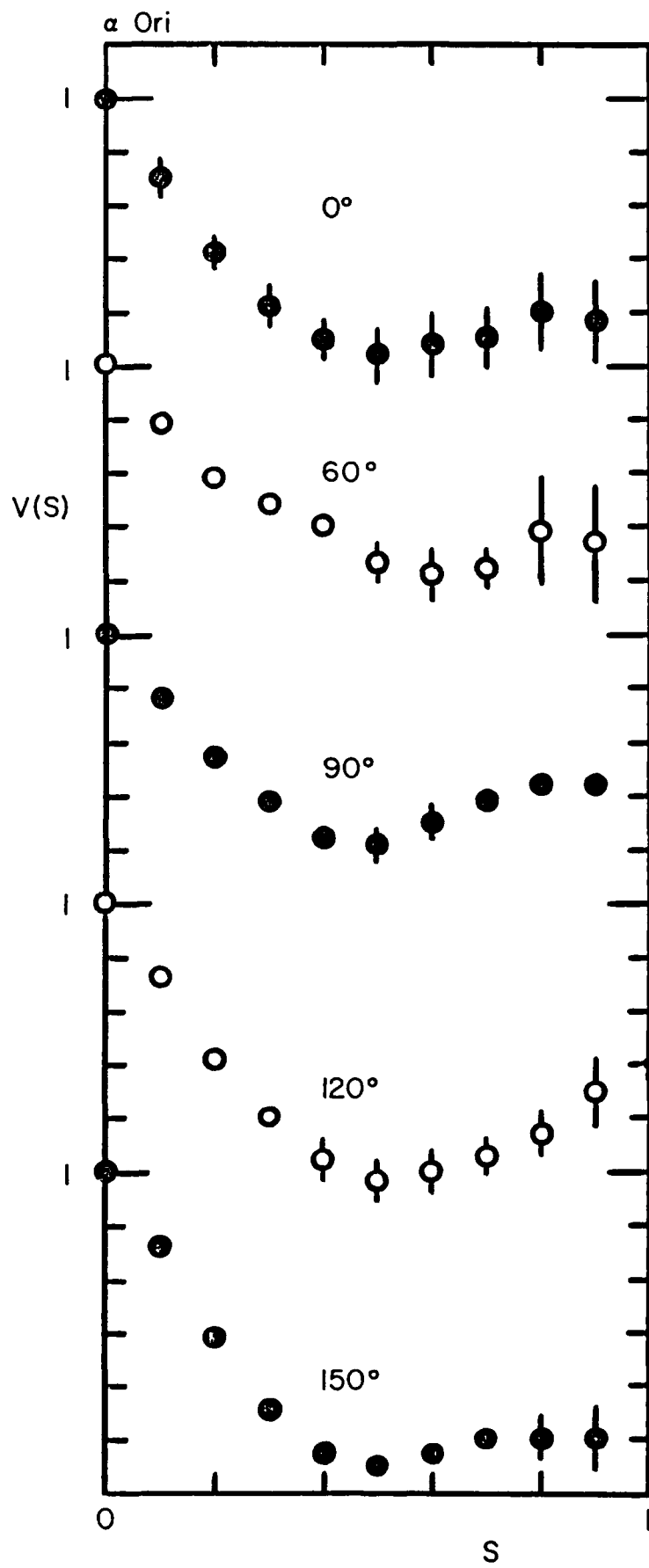
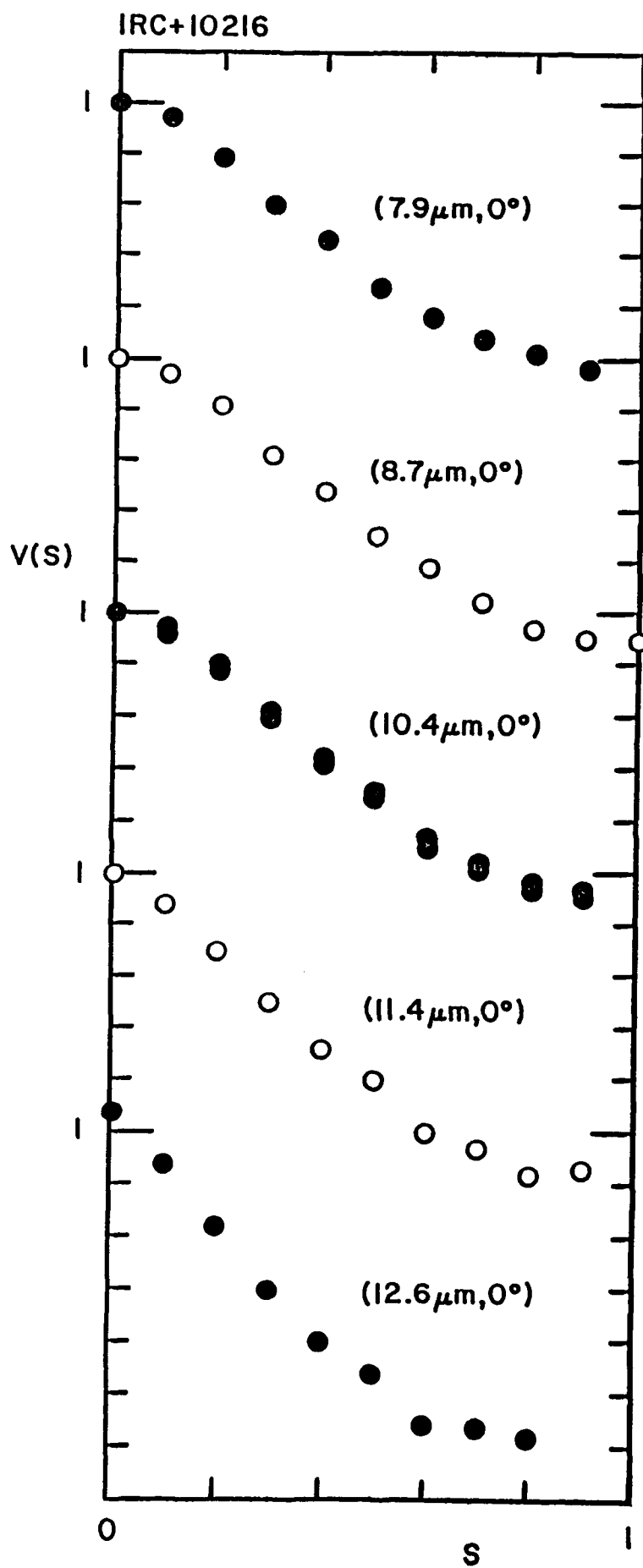


FIGURE A11





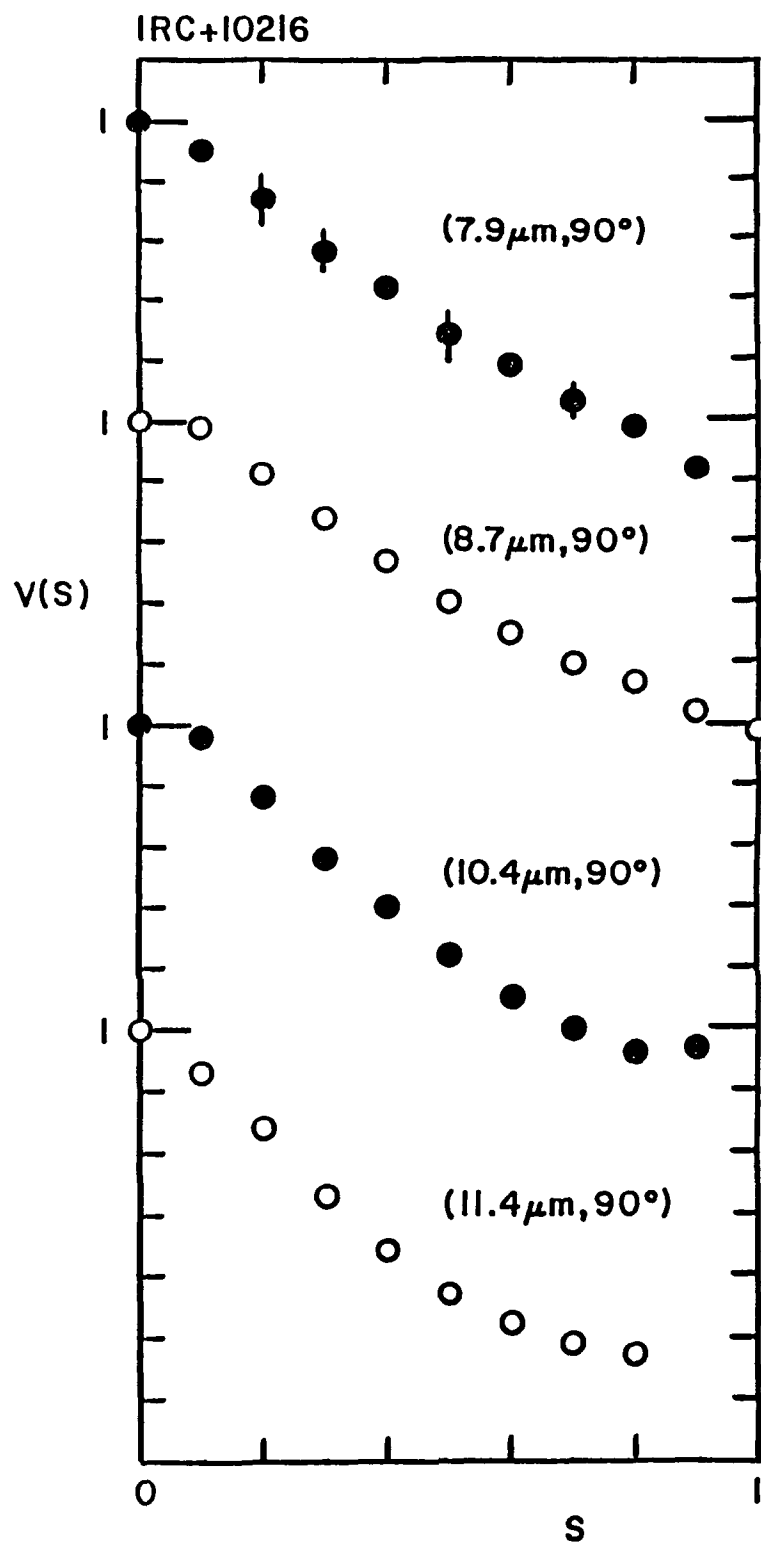


FIGURE A14

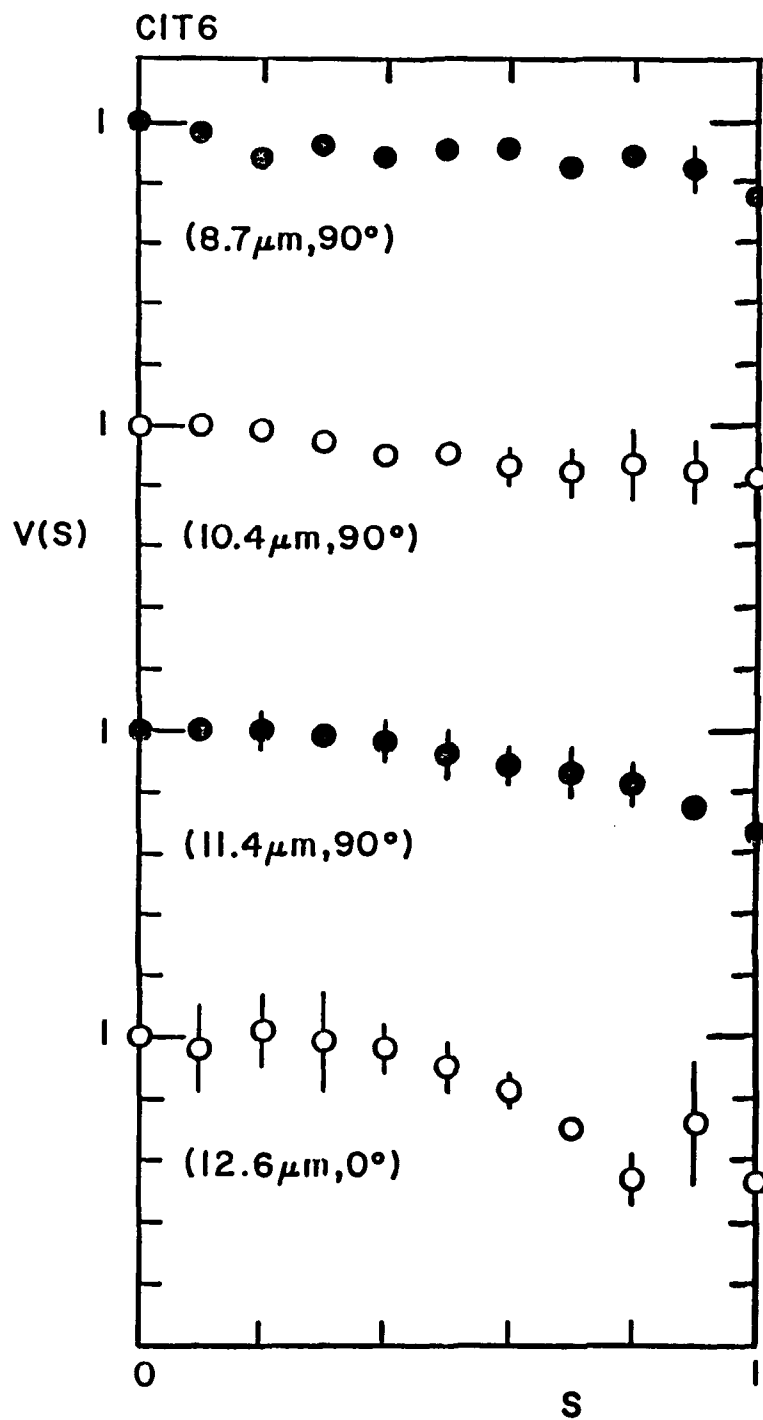


FIGURE A15

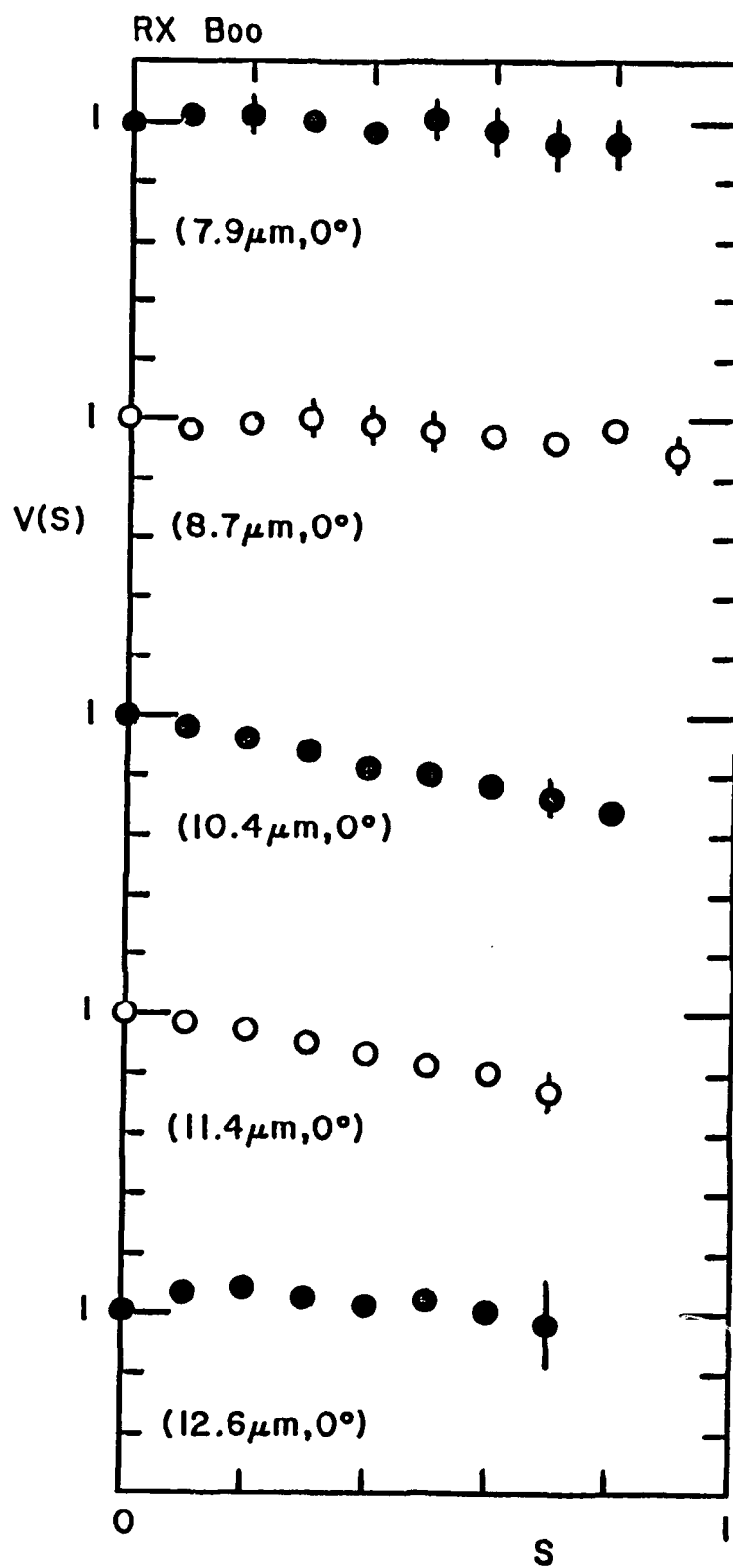


FIGURE A16

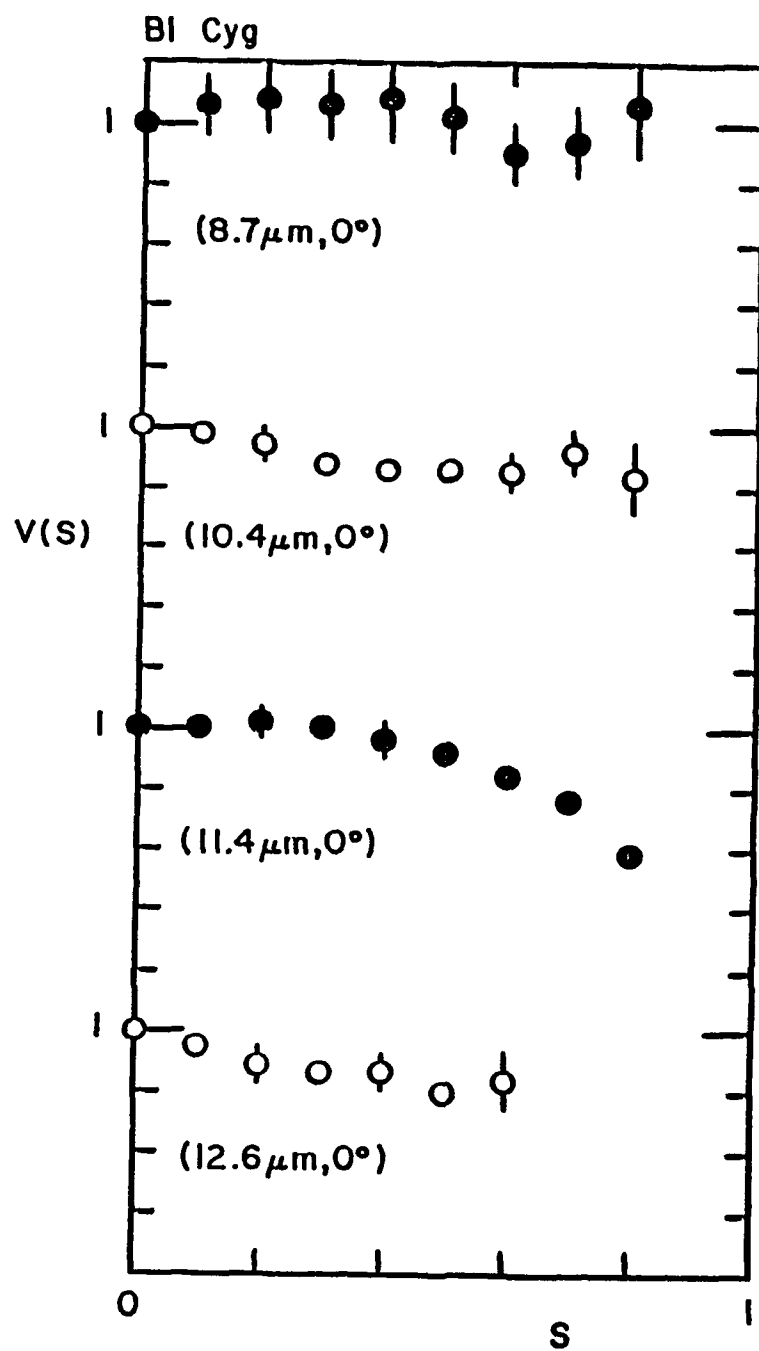


FIGURE A17

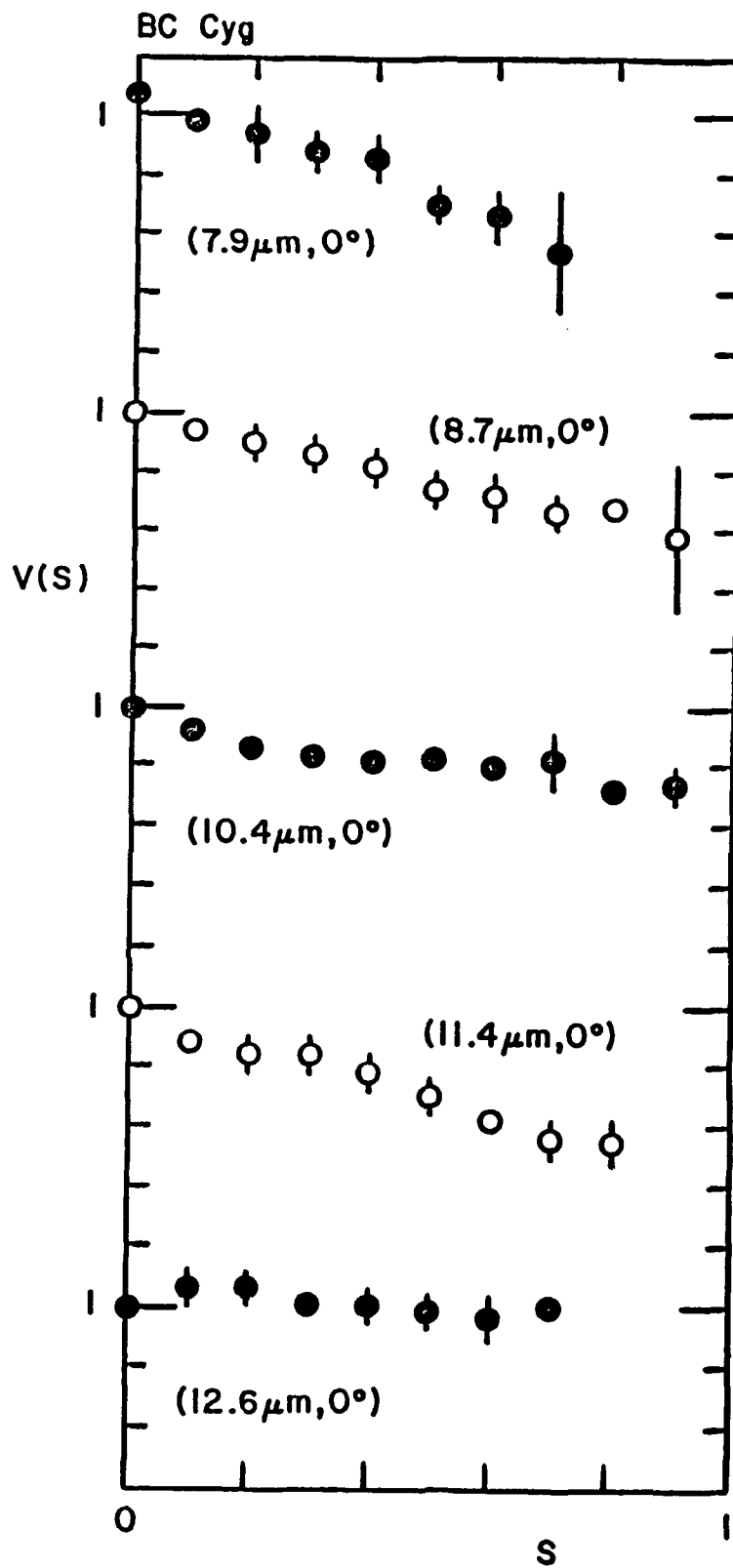


FIGURE A13

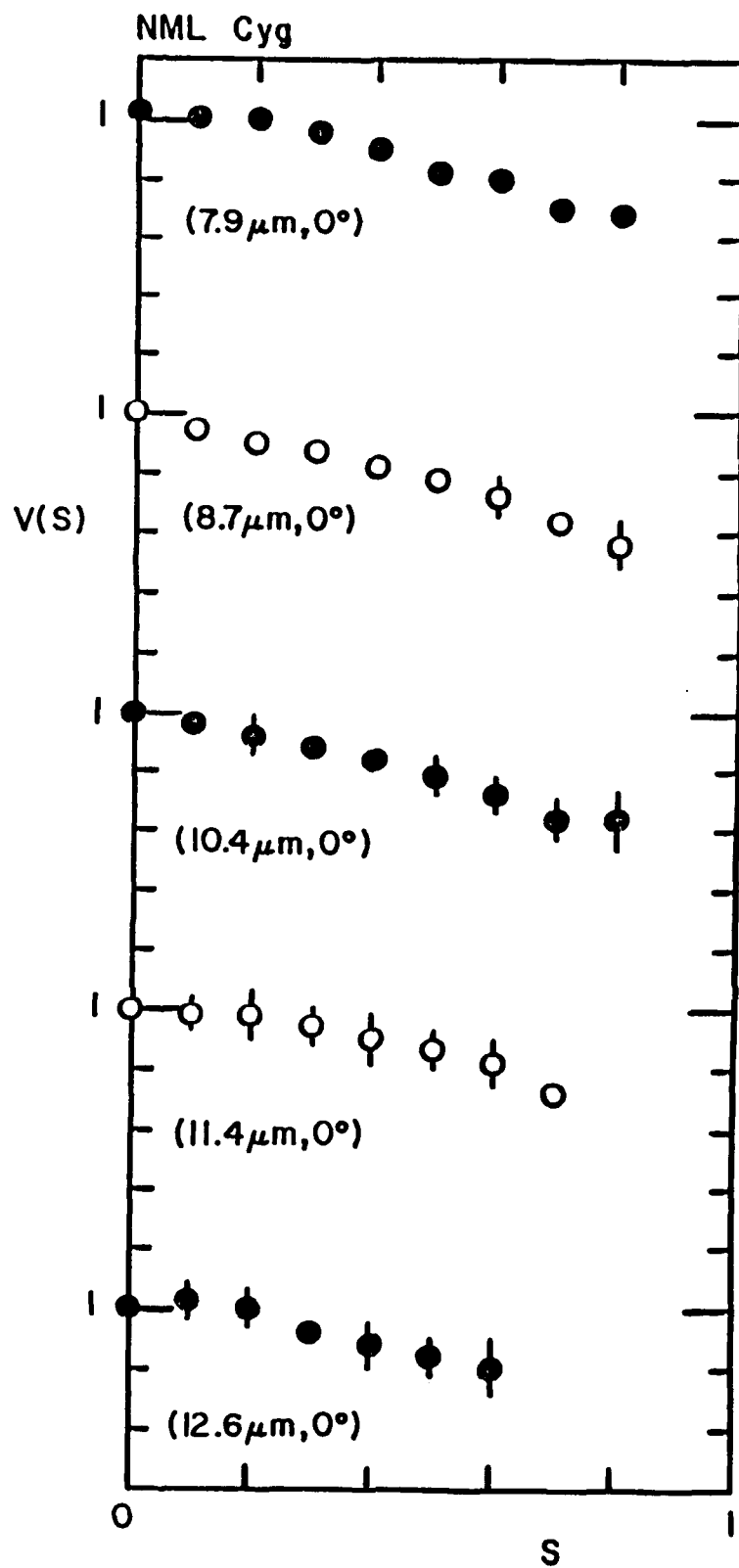
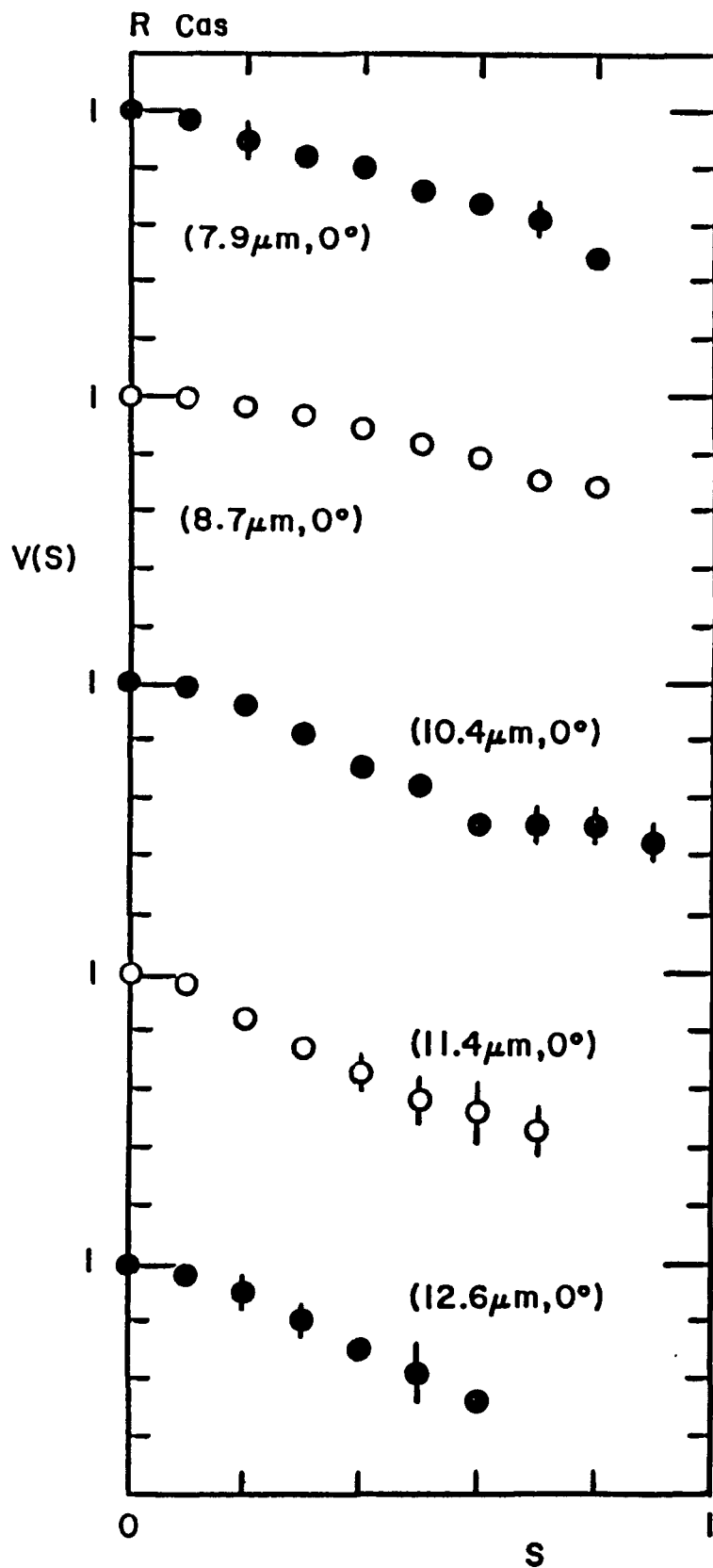


FIGURE A19



Approved for release by NSA on 09-10-2013 pursuant to E.O. 13526

FIGURE A20